4. Discontinuous Galerkin methods for elastoplasticity

Until this point only elasticity has been considered. The main objective of this chapter is to extend the formulation of the interior penalty method to the plasticity case obtaining a consistent and stable discontinuous method. Going back to the primal formulation of the interior penalty method in equation (3.14), it might seem logical to think that the weak form for the plasticity case is obtained by substitution of $\mathbf{C} : \nabla^s \boldsymbol{u}^h$ by $\boldsymbol{\sigma}^h$. However the treatment of the symmetry term becomes ambiguous. This problem will be solved in two steps, in Section 4.1 the consistent non-symmetric discontinuous Galerkin method will be derived for plasticity. Once this has been done, in Section 4.2 a term will be added to obtain a symmetric and consistent method.

4.1. Non-symmetric discontinuous Galerkin method

4.1.1. Weak form of non-symmetrical discontinuous Galerkin method

We consider the same problem as in Section 2.2. The local equilibrium equation in (2.7) holds as well for plasticity, however, now the constitutive equation in (2.8) is no longer valid. A new constitutive equation relating the rate of stresses and strains and depending on the plasticity model adopted will be used.

Since equation (2.27) has been obtained through integration by parts of the local equilibrium equation in (2.7) and this is still valid for plasticity, equation (2.27) can still be used now. Again it is considered that $\boldsymbol{g}^D = \mathbf{0}$. For the non-symmetric discontinuous Galerkin method the numerical fluxes used for plasticity are the same as in elasticity, equations (3.15)–(3.18), only changing the definition of $\hat{\boldsymbol{\sigma}}$ in equation (3.17), where $\left\{\mathbf{C} : \nabla^s \boldsymbol{u}^h\right\}$ is substituted by $\left\{\boldsymbol{\sigma}^h\right\}$,

$$\hat{\boldsymbol{\sigma}} \boldsymbol{n}_K = \left\{\boldsymbol{\sigma}^h\right\} \boldsymbol{n}_K - \boldsymbol{\mu} \left[\!\left[\boldsymbol{u}^h\right]\!\right] \qquad \text{on } \tilde{\Gamma} \cup \Gamma^D. \tag{4.1}$$

Introducing these numerical fluxes into equation (2.27) the primal form is obtained,

$$\int_{\tilde{\Omega}} \nabla^s \boldsymbol{\omega}^h : \boldsymbol{\sigma}^h d\Omega - \int_{\tilde{\Gamma}} \left[\!\left[\boldsymbol{\omega}^h\right]\!\right] \cdot \left\{\boldsymbol{\sigma}^h\right\} \boldsymbol{n}_K d\Gamma + \int_{\tilde{\Gamma}} \left[\!\left[\boldsymbol{\omega}^h\right]\!\right] \frac{\eta_K}{h_K} \boldsymbol{D} \left[\!\left[\boldsymbol{u}^h\right]\!\right] d\Gamma = \int_{\tilde{\Omega}} \boldsymbol{\omega}^h \cdot \boldsymbol{f} d\Omega + \int_{\Gamma^N} \boldsymbol{\omega}^h \cdot \boldsymbol{g}^N d\Gamma. \tag{4.2}$$

This is the nonlinear equation that will be solved through an incremental iterative procedure in the next two sections. The definition of $\boldsymbol{\mu} = \frac{\eta_K}{h_K} \boldsymbol{D}$ given for elasticity in equation (3.13) remains unchanged for plasticity. This is because $\boldsymbol{\mu}$ has no real physical meaning for the non-symmetric discontinuous Galerkin method and only acts as a penalty. Any value of $\boldsymbol{\mu}$ is therefore valid, as long as the stability condition in equation (2.47) is satisfied. The

chosen value of $\boldsymbol{D}$ can be seen in equation (3.40) for the one dimensional case and in (3.47) for two dimensions.

See that the method is consistent since the numerical fluxes are consistent. However in this case, and unlike the IP method, it is not adjoint consistent. The value of $\hat{u}$ takes a different value at each side of $\tilde{\Gamma}$, $\boldsymbol{u}^h_{\partial K_1}$ over ∂K_1 and $\boldsymbol{u}^h_{\partial K_2}$ over ∂K_2, see figure 3.1.

From this point, and to derive the incremental iterative procedure that will solve the plasticity problem, there are two steps that need to be followed. These are the discretization of the weak form, and then its linearization. The order on which this is done does not affect the result. In this case discretization will be done first, followed by the linearization.

4.1.2. Spatial discretization of non-symmetric discontinuous Galerkin method

Using the defined notation in Section 3.5, equation (4.2) can be discretized for the interface element in figure 3.1 as,

$$\begin{aligned}\int_{K_1} (\mathbf{B}_{e_1})^T \boldsymbol{\sigma}^h_{e_1} d\Omega + \int_{K_2} (\mathbf{B}_{e_2})^T \boldsymbol{\sigma}^h_{e_2} d\Omega - \int_{\tilde{\Gamma}} \left(\mathbf{N}_o^{[\![\,]\!]}\right)^T \left\{\boldsymbol{\sigma}^h\right\} \boldsymbol{n}_K d\Gamma \\ + \int_{\tilde{\Gamma}} \left(\mathbf{N}_o^{[\![\,]\!]}\right)^T \frac{\eta_K}{h_K} \boldsymbol{D}\, \mathbf{N}_o^{[\![\,]\!]} \mathbf{a}_o \, d\Gamma = \int_{K_1} (\mathbf{N}_{e_1})^T \boldsymbol{f} d\Omega + \int_{K_2} (\mathbf{N}_{e_2})^T \boldsymbol{f} d\Omega \\ + \int_{\Gamma^N} (\mathbf{N}_e)^T \boldsymbol{g}^N d\Gamma. \quad (4.3)\end{aligned}$$

From the above expression the global equilibrium condition can be obtained,

$$\mathbf{F}_{\text{ext}} - \mathbf{F}_{\text{int}} = 0, \quad (4.4)$$

where,

$$\begin{aligned}\mathbf{F}_{\text{int}} = \int_{K_1} (\mathbf{B}_{e_1})^T \boldsymbol{\sigma}^h_{e_1} d\Omega + \int_{K_2} (\mathbf{B}_{e_2})^T \boldsymbol{\sigma}^h_{e_2} d\Omega - \int_{\tilde{\Gamma}} \left(\mathbf{N}_o^{[\![\,]\!]}\right)^T \left\{\boldsymbol{\sigma}^h\right\} \boldsymbol{n}_K d\Gamma \\ + \int_{\tilde{\Gamma}} \left(\mathbf{N}_o^{[\![\,]\!]}\right)^T \frac{\eta_K}{h_K} \boldsymbol{D}\, \mathbf{N}_o^{[\![\,]\!]} \mathbf{a}_o \, d\Gamma, \quad (4.5)\end{aligned}$$

and

$$\mathbf{F}_{\text{ext}} = \int_{K_1} (\mathbf{N}_{e_1})^T \boldsymbol{f} d\Omega + \int_{K_2} (\mathbf{N}_{e_2})^T \boldsymbol{f} d\Omega + \int_{\Gamma^N} (\mathbf{N}_e)^T \boldsymbol{g}^N d\Gamma. \quad (4.6)$$

The equilibrium expression in (4.4) states that the internal virtual work, $\mathbf{F}_{\text{int}}$, of the stresses and contributions from interior boundaries, is equal to the external virtual work, $\mathbf{F}_{\text{ext}}$, of the boundary tractions $\boldsymbol{g}^N$ and body forces $\boldsymbol{f}$ [14].

4.1.3. Linearization of non-symmetric discontinuous Galerkin method

The problem is now reduced to finding an $\Delta \boldsymbol{u}^{h\,(k+1)}$ so that the updated displacements, strains and stresses satisfy the equilibrium equation in (4.4) for a given level of load n, and the calculated stresses lie within the permissible limits of the used yield surface.

The solution to this problem is obtained through an incremental-iterative procedure, where the superscript k will be used to express the iteration number. Since the displacement and strains have already been discretized in Section 4.1.2, instead of $\boldsymbol{u}^{h\ (k+1)}$, nodal displacements will be used, $\mathbf{a}^{(k+1)}$. The steps to be followed are mainly,

1. Given a trial displacement increment update the nodal displacements,

$$\mathbf{a}_e^{(k+1)} = \mathbf{a}_e^{(k)} + \Delta\mathbf{a}_e^{(k+1)}, \tag{4.7}$$

   and with $\mathbf{a}_e^{(k+1)}$ update the strains for each quadrature point,

$$\boldsymbol{\varepsilon}_e^{(k+1)} = \mathbf{B}_e\ \mathbf{a}_e^{(k+1)}. \tag{4.8}$$

   In the interior boundaries, the strains can be computed just by evaluating $\mathbf{B}_e$ on each of the sides of $\tilde{\Gamma}$, ∂K_1 and ∂K_2, figure 3.1,

$$\boldsymbol{\varepsilon}_{\partial K}^{(k+1)} = \mathbf{B}_e|_{\partial K}\ \mathbf{a}_e^{(k+1)}. \tag{4.9}$$

2. For each quadrature point, given the strain field, $\boldsymbol{\varepsilon}_e^{(k+1)}$, the plastic strain $\boldsymbol{\varepsilon}_e^{p\ (k+1)}$ and hardening variables $\boldsymbol{q}_e^{(k+1)}$ the corresponding stress $\boldsymbol{\sigma}_e^{(k+1)}$ is computed using a classical return mapping algorithm. The same is done on ∂K_1 and ∂K_2 with $\boldsymbol{\varepsilon}_{\partial K}^{(k+1)}$, $\boldsymbol{\varepsilon}_{\partial K}^{p\ (k+1)}$ and $\boldsymbol{q}_{\partial K}^{(k+1)}$ to obtain $\boldsymbol{\sigma}_{\partial K}^{(k+1)}$.

3. With $\boldsymbol{\sigma}_e^{(k+1)}$, $\boldsymbol{\sigma}_{\partial K}^{(k+1)}$ and $\mathbf{a}_o^{(k+1)}$ evaluate $\mathbf{F}_{\text{int}}^{(k+1)}$ using expression (4.5).

4. For the given load level, $\boldsymbol{f}^{\ (n)}$ and $\boldsymbol{g}^{N\ (n)}$, evaluate $\mathbf{F}_{\text{ext}}^{(n)}$ using (4.6).

5. Check if the equilibrium equation in (4.4) is satisfied. If this is the case the solution for the corresponding load level n has been found, go then to the next load level $n+1$. If this is not the case, continue.

6. Calculate the following displacement increment, set $k+1$ equal to k and go back to point one until the equilibrium equation (4.4) holds.

The only step which is not yet clear is the last one. What happens if after an increment the equilibrium expression in (4.4) is not satisfied, and how is the following increment calculated? Here, to determine this last step, and following [1], $\Delta\mathbf{a}_e^{(k+1)}$ will be obtained by linearizing the expression of $\mathbf{F}_{\text{int}}$, in equation (4.5), around the current state, $\mathbf{a}_e^{(k+1)}$, so that the equilibrium equation (4.4) can be rewritten as,

$$\mathbf{F}_{\text{ext}}^{(n)} - \mathbf{F}_{\text{int}}^{(k)} - \frac{\partial \mathbf{F}_{\text{int}}}{\partial \mathbf{a}^{(k+1)}}\Delta\mathbf{a}^{(k+1)} = 0, \tag{4.10}$$

where,

$$\frac{\partial \mathbf{F}_{\text{int}}}{\partial \mathbf{a}_e^{(k+1)}} \Delta \mathbf{a}_e^{(k+1)} = \int_{K_1} (\mathbf{B}_{e_1})^T \frac{\partial \boldsymbol{\sigma}_{e_1}^h}{\partial \mathbf{a}_{e_1}^{(k+1)}} \Delta \mathbf{a}_{e_1}^{(k+1)} d\Omega + \int_{K_2} (\mathbf{B}_{e_2})^T \frac{\partial \boldsymbol{\sigma}_{e_2}^h}{\partial \mathbf{a}_{e_2}^{(k+1)}} \Delta \mathbf{a}_{e_2}^{(k+1)} d\Omega$$
$$- \int_{\tilde{\Gamma}} \left(\mathbf{N}_o^{[\![\,]\!]} \right)^T \frac{\partial \left(\left\{ \boldsymbol{\sigma}^h \right\} \boldsymbol{n}_K \right)}{\partial \mathbf{a}_o^{(k+1)}} \Delta \mathbf{a}_o^{(k+1)} d\Gamma + \int_{\tilde{\Gamma}} \left(\mathbf{N}_o^{[\![\,]\!]} \right)^T \frac{\eta_K}{h_K} \boldsymbol{D}\, \mathbf{N}_o^{[\![\,]\!]} \frac{\partial \mathbf{a}_o}{\partial \mathbf{a}_o^{(k+1)}} \Delta \mathbf{a}_o^{(k+1)}\, d\Gamma. \tag{4.11}$$

Now the problem is reduced to obtaining an expression of the stress increment as a function of the displacement, so that the derivations in the first, second and third term of the left hand side of the above equation can be calculated. Consider the constitutive equation for the elastic case in (2.8). For plasticity this is not valid anymore since the tangent modulus is not constant. However for a given infinetly small strain increment it holds that,

$$\dot{\boldsymbol{\sigma}} = \mathbf{C}^{\text{ep}} : \nabla^s \dot{\boldsymbol{u}}, \tag{4.12}$$

where,

$$\dot{(\cdot)} = \frac{\partial (\cdot)}{\partial t}. \tag{4.13}$$

This infinetly small increment can be seen as a variation of the analyzed variable during a small period of fictitious time. This notation will be used to refer to small changes. In fact being more consistent the notation used should have been $\delta(\cdot) = \dot{(\cdot)}\delta t$. However for simplicity, and because it is an extended notation used in plasticity theory $\dot{(\cdot)}$ will express a small change [1].

In order to proceed with the linearization, a definition of $\dot{\boldsymbol{\sigma}}^h$ over $\tilde{\Omega}$ is required. As done for the elasticity case to obtain equation (2.31) through integration by parts of the constitutive equation (2.8) to obtain equation (3.59) but now starting from (4.12) it yields,

$$\int_{\tilde{\Omega}} \nabla^s \boldsymbol{\omega}^h : \dot{\boldsymbol{\sigma}}^h d\Omega = \int_{\tilde{\Omega}} \nabla^s \boldsymbol{\omega}^h : \mathbf{C}^{\text{ep}} : \nabla^s \dot{\boldsymbol{u}}^h d\Omega - \int_{\tilde{\Gamma} \cup \Gamma} \left\{ \nabla^s \boldsymbol{\omega}^h : \mathbf{C}^{\text{ep}} \right\} \boldsymbol{n}_K \cdot \left[\!\left[\dot{\boldsymbol{u}}^h \right]\!\right] d\Gamma$$
$$- \int_{\tilde{\Gamma}} \left[\!\left[\nabla^s \boldsymbol{\omega}^h : \mathbf{C}^{\text{ep}} \right]\!\right] \boldsymbol{n}_K \cdot \left\{ \dot{\boldsymbol{u}}^h \right\} d\Gamma + \int_{\tilde{\Gamma} \cup \Gamma} \left\{ \nabla^s \boldsymbol{\omega}^h : \mathbf{C}^{\text{ep}} \right\} \boldsymbol{n}_K \cdot \left[\!\left[\hat{\dot{\boldsymbol{u}}} \right]\!\right] d\Gamma$$
$$+ \int_{\tilde{\Gamma}} \left[\!\left[\nabla^s \boldsymbol{\omega}^h : \mathbf{C}^{\text{ep}} \right]\!\right] \boldsymbol{n}_K \cdot \left\{ \hat{\dot{\boldsymbol{u}}} \right\} d\Gamma. \tag{4.14}$$

For an infinetly small increment the numerical fluxes in (3.15) and (3.16) are expressed as,

$$\hat{\dot{\boldsymbol{u}}} = \dot{\boldsymbol{u}}_{\partial K}^h \qquad \text{on } \tilde{\Gamma} \cup \Gamma^N, \tag{4.15}$$
$$\hat{\dot{\boldsymbol{u}}} = \mathbf{0} \qquad \text{on } \Gamma^D, \tag{4.16}$$

where $\boldsymbol{g}^D$ has been considered equal to $\boldsymbol{g}^D = \mathbf{0}$. So equation (4.14) reduces to,

$$\int_{\tilde{\Omega}} \nabla^s \boldsymbol{\omega}^h : \dot{\boldsymbol{\sigma}}^h d\Omega = \int_{\tilde{\Omega}} \nabla^s \boldsymbol{\omega}^h : \mathbf{C}^{\text{ep}} : \nabla^s \dot{\boldsymbol{u}}^h d\Omega. \tag{4.17}$$

Since this holds for any $\boldsymbol{\omega}^h \in \mathcal{W}^h$, it follows,

$$\dot{\boldsymbol{\sigma}}^h = \mathbf{C}^{\text{ep}} : \nabla^s \dot{\boldsymbol{u}}^h \qquad \text{in } \tilde{\Omega}. \tag{4.18}$$

Going now back to equation (4.11), the linearization of the first term of the left hand side is, see [1],

$$\int_{K_1} (\mathbf{B}_{e_1})^T \frac{\partial \boldsymbol{\sigma}^h_{e_1}}{\partial \mathbf{a}^{(k+1)}_{e_1}} \Delta \mathbf{a}^{(k+1)}_{e_1} d\Omega = \int_{K_1} (\mathbf{B}_{e_1})^T \frac{\partial \boldsymbol{\sigma}^h_{e_1}}{\partial \boldsymbol{\varepsilon}^{(k+1)}_{e_1}} \frac{\partial \boldsymbol{\varepsilon}^{(k+1)}_{e_1}}{\partial \mathbf{a}^{(k+1)}_{e_1}} \Delta \mathbf{a}^{(k+1)}_{e_1} d\Omega, \tag{4.19}$$

from expression (4.18) it follows that in $\tilde{\Omega}$,

$$\frac{\partial \boldsymbol{\sigma}^h_{e_1}}{\partial \boldsymbol{\varepsilon}^{(k+1)}_{e_1}} = \mathbf{C}^{\text{ep}\ (k+1)}_{e_1} \qquad \text{in } K_1, \tag{4.20}$$

and from equation (4.8),

$$\frac{\partial \boldsymbol{\varepsilon}^{(k+1)}_{e_1}}{\partial \mathbf{a}^{(k+1)}_{e_1}} = \mathbf{B}_{e_1}. \tag{4.21}$$

In expression (4.20) the elastoplastic modulus $\mathbf{C}^{\text{ep}\ (k+1)}_{e_1}$ will be written as $\mathbf{C}^{\text{ep}}_{e_1}$ to simplify the notation. It has to be remembered however that it is not constant for every iteration nor for every Gauss point. So with equations (4.20) and (4.21) expression (4.19) yields,

$$\int_{K_1} (\mathbf{B}_{e_1})^T \frac{\partial \boldsymbol{\sigma}^h_{e_1}}{\partial \mathbf{a}^{(k+1)}_{e_1}} \Delta \mathbf{a}^{(k+1)}_{e_1} d\Omega = \int_{K_1} (\mathbf{B}_{e_1})^T \mathbf{C}^{\text{ep}}_{e_1} \mathbf{B}_{e_1}\, d\Omega\ \Delta \mathbf{a}^{(k+1)}_{e_1}. \tag{4.22}$$

This procedure is completely analogous to the one that must be followed with the second term of (4.11), but instead of over K_1, now over K_2, see figure 3.1.

With the third term of the linearized equation in (4.11), and due to the linearity of the average operator, using equation (4.20) and (4.21) it yields,

$$\begin{aligned}\int_{\tilde{\Gamma}} \left(\mathbf{N}^{[\![\ ]\!]}_o\right)^T \frac{\partial \left(\left\{\boldsymbol{\sigma}^h\right\} \boldsymbol{n}_K\right)}{\partial \mathbf{a}^{(k+1)}_o} \Delta \mathbf{a}^{(k+1)}_o d\Gamma &= \int_{\tilde{\Gamma}} \left(\mathbf{N}^{[\![\ ]\!]}_o\right)^T \frac{\partial \left\{\boldsymbol{\sigma}^h \boldsymbol{n}_K\right\}}{\partial \mathbf{a}^{(k+1)}_o} \Delta \mathbf{a}^{(k+1)}_o d\Gamma \\ &= \int_{\tilde{\Gamma}} \left(\mathbf{N}^{[\![\ ]\!]}_o\right)^T \frac{1}{2} \left(\frac{\partial \boldsymbol{\sigma}^h_{\partial K_1} \boldsymbol{n}_K}{\partial \mathbf{a}^{(k+1)}_{e_1}} \Delta \mathbf{a}^{(k+1)}_{e_1} + \frac{\partial \boldsymbol{\sigma}^h_{\partial K_2} \boldsymbol{n}_K}{\partial \mathbf{a}^{(k+1)}_{e_2}} \Delta \mathbf{a}^{(k+1)}_{e_2} \right) d\Gamma,\end{aligned} \tag{4.23}$$

again from expression (4.18),

$$\frac{\partial \boldsymbol{\sigma}^h_{\partial K_1}}{\partial \boldsymbol{\varepsilon}^{(k+1)}_{e_1}} = \mathbf{C}^{\text{ep}\ (k+1)}_{\partial K_1} \qquad \text{in } \partial K_1, \tag{4.24}$$

and considering again equation (4.21), expression (4.23) yields

$$\begin{aligned}
&\int_{\tilde{\Gamma}} \left(\mathbf{N}_o^{[\![\,]\!]}\right)^T \frac{1}{2}\left(\frac{\partial \boldsymbol{\sigma}^h_{\partial K_1}\boldsymbol{n}_K}{\partial \mathbf{a}_{e_1}^{(k+1)}}\Delta\mathbf{a}_{e_1}^{(k+1)} + \frac{\partial \boldsymbol{\sigma}^h_{\partial K_2}\boldsymbol{n}_K}{\partial \mathbf{a}_{e_2}^{(k+1)}}\Delta\mathbf{a}_{e_2}^{(k+1)}\right) d\Gamma \\
&= \int_{\tilde{\Gamma}} \left(\mathbf{N}_o^{[\![\,]\!]}\right)^T \frac{1}{2}\left(\mathbf{C}^{\text{ep}}_{\partial K_1}\mathbf{B}_{e_1}\boldsymbol{n}_K\Delta\mathbf{a}_{e_1}^{(k+1)} + \mathbf{C}^{\text{ep}}_{\partial K_2}\mathbf{B}_{e_2}\boldsymbol{n}_K\Delta\mathbf{a}_{e_2}^{(k+1)}\right) d\Gamma \\
&= \int_{\tilde{\Gamma}} \left(\mathbf{N}_o^{[\![\,]\!]}\right)^T \frac{1}{2}\left[\begin{array}{cc} \mathbf{C}^{\text{ep}}_{\partial K_1}\mathbf{B}_{e_1}\boldsymbol{n}_K & \mathbf{C}^{\text{ep}}_{\partial K_2}\mathbf{B}_{e_2}\boldsymbol{n}_K \end{array}\right] d\Gamma\ \Delta\mathbf{a}_o^{(k+1)} \\
&\qquad = \int_{\tilde{\Gamma}} \left(\mathbf{N}_o^{[\![\,]\!]}\right)^T \mathbf{B}_o^{\{\mathbf{C}^{\text{ep}}\}} d\Gamma\ \Delta\mathbf{a}_o^{(k+1)}, \quad (4.25)
\end{aligned}$$

where the term $\mathbf{B}_o^{\{\mathbf{C}^{\text{ep}}\}}$ is calculated as in Appendix B, but now, instead of using the elastic tangent matrix $\mathbf{C}$, use is made of the elastoplastic tangent modulus at both sides of $\tilde{\Gamma}$, $\mathbf{C}^{\text{ep}}_{\partial K_1}$ and $\mathbf{C}^{\text{ep}}_{\partial K_2}$.

For the last term of the linearized form of $\mathbf{F}_{\text{int}}$ in equation (4.11) it automatically follows,

$$\int_{\tilde{\Gamma}} \left(\mathbf{N}_o^{[\![\,]\!]}\right)^T \frac{\eta_K}{h_K}\boldsymbol{D}\,\mathbf{N}_o^{[\![\,]\!]}\frac{\partial \mathbf{a}_o}{\partial \mathbf{a}_o^{(k+1)}}\Delta\mathbf{a}_o^{(k+1)}\, d\Gamma = \int_{\tilde{\Gamma}} \left(\mathbf{N}_o^{[\![\,]\!]}\right)^T \frac{\eta_K}{h_K}\boldsymbol{D}\,\mathbf{N}_o^{[\![\,]\!]} d\Gamma\ \Delta\mathbf{a}_o^{(k+1)}. \quad (4.26)$$

Going now back to equation (4.10), to calculate $\Delta\mathbf{a}^{(k+1)}$ the following system will be solved,

$$\mathbf{K}^{(k+1)}\Delta\mathbf{a}^{(k+1)} = \mathbf{F}_{\text{ext}}^{(n)} - \mathbf{F}_{\text{int}}^{(k)}, \quad (4.27)$$

being $\mathbf{K}^{(k+1)}$ the global stiffness matrix, obtained by assembling the corresponding contributions of equations (4.22), (4.25) and (4.26) from each of the two elements and the interior boundary of figure 3.1,

$$\mathbf{K}_o^{(k+1)} = \left[\begin{array}{c} \int_{K_1}\mathbf{B}_{e_1}^T\mathbf{C}^{\text{ep}}_{e_1}\mathbf{B}_{e_1}d\Omega \\ \int_{K_2}\mathbf{B}_{e_2}^T\mathbf{C}^{\text{ep}}_{e_2}\mathbf{B}_{e_2}d\Omega \end{array}\right] - \int_{\tilde{\Gamma}} \left(\mathbf{N}_o^{[\![\,]\!]}\right)^T \mathbf{B}_o^{\{\mathbf{C}^{\text{ep}}\}} d\Gamma + \int_{\tilde{\Gamma}} \left(\mathbf{N}_o^{[\![\,]\!]}\right)^T \frac{\eta_K}{h_K}\boldsymbol{D}\,\mathbf{N}_o^{[\![\,]\!]} d\Gamma, \quad (4.28)$$

$$\mathbf{F}_{\text{ext}}^{(n)} = \left[\begin{array}{c} \int_{K_1}\left(\mathbf{N}_{e_1}\right)^T\boldsymbol{f}^{(n)}d\Omega \\ \int_{K_2}\left(\mathbf{N}_{e_2}\right)^T\boldsymbol{f}^{(n)}d\Omega \end{array}\right] + \int_{\Gamma^N}\mathbf{N}_e^T\boldsymbol{g}^{N\,(n)}d\Gamma, \quad (4.29)$$

$$\begin{aligned}
\mathbf{F}_{\text{int}}^{(k)} = &\left[\begin{array}{c} \int_{K_1}\mathbf{B}_{e_1}^T\boldsymbol{\sigma}_{e_1}^{h\,(k)}\,d\Omega \\ \int_{K_2}\mathbf{B}_{e_2}^T\boldsymbol{\sigma}_{e_2}^{h\,(k)}\,d\Omega \end{array}\right] - \int_{\tilde{\Gamma}} \left(\mathbf{N}_o^{[\![\,]\!]}\right)^T \left\{\boldsymbol{\sigma}^{h\,(k)}\right\} d\Gamma \\
&+ \int_{\tilde{\Gamma}} \left(\mathbf{N}_o^{[\![\,]\!]}\right)^T \frac{\eta_K}{h_K}\boldsymbol{D}\,\mathbf{N}_o^{[\![\,]\!]} d\Gamma\ \mathbf{a}_o^{(k)}. \quad (4.30)
\end{aligned}$$

The obtained method is consistent, however an important drawback is that the rate of convergence is not optimal, as seen in elasticity. Another disadvantage is that the resulting stiffness matrix is not symmetric.

4.2. Interior penalty method

A term will now be added that restores symmetry to the method and does not affect the consistency. However, as will be seen, this is not straightforward, and some assumptions will have to be made.

4.2.1. Weak form of interior penalty Method

The numerical fluxes in equations (3.1), (3.2) and (3.4) remain unchanged, and only the numerical flux in equation (3.3) changes into,

$$\hat{\boldsymbol{\sigma}}\boldsymbol{n}_K = \left\{\boldsymbol{\sigma}^h_{\text{int}}\right\}\boldsymbol{n}_K - \boldsymbol{\mu}\left[\!\left[\boldsymbol{u}^h\right]\!\right] \qquad \text{on } \tilde{\Gamma} \cup \Gamma^D. \tag{4.31}$$

Again $\boldsymbol{g}^D = \boldsymbol{0}$. Note that if the real solution $\boldsymbol{u}$ is substituted into equation (4.31), $\boldsymbol{\sigma}_{\text{bound}} = \boldsymbol{0}$ and it yields,

$$\boldsymbol{\sigma} = \boldsymbol{\sigma}_{\text{int}}, \tag{4.32}$$

so finally,

$$\hat{\boldsymbol{\sigma}}(\boldsymbol{u})\boldsymbol{n}_K = \{\boldsymbol{\sigma}_{\text{int}}\}\boldsymbol{n}_K - \boldsymbol{\mu}[\![\boldsymbol{u}]\!] = \boldsymbol{\sigma}\boldsymbol{n}_K \qquad \text{on } \tilde{\Gamma} \cup \Gamma^D. \tag{4.33}$$

As in the elastic case, a consistent and conservative numerical fluxes is obtained. The used value of $\boldsymbol{\mu}$ is the same as in the elastic case, see equations (3.40) and (3.47).

The weak form to be solved can be obtained by inserting the new numerical fluxes into equation (2.27) to obtain,

$$\int_{\tilde{\Omega}} \nabla^s \boldsymbol{\omega}^h : \boldsymbol{\sigma}^h d\Omega - \int_{\tilde{\Gamma}} \left[\!\left[\boldsymbol{\omega}^h\right]\!\right] \cdot \left\{\boldsymbol{\sigma}^h_{\text{int}}\right\} \boldsymbol{n}_K d\Gamma + \int_{\tilde{\Gamma}} \left[\!\left[\boldsymbol{\omega}^h\right]\!\right] \frac{\eta_K}{h_K} \boldsymbol{D} \left[\!\left[\boldsymbol{u}^h\right]\!\right] d\Gamma$$
$$= \int_{\tilde{\Omega}} \boldsymbol{\omega}^h \cdot \boldsymbol{f} d\Omega + \int_{\Gamma^N} \boldsymbol{\omega}^h \cdot \boldsymbol{g}^N d\Gamma. \tag{4.34}$$

In order to solve equation (4.34) an expression must be given between $\boldsymbol{\sigma}^h$ and $\boldsymbol{\sigma}^h_{\text{int}}$. However the definition given for $\boldsymbol{\sigma}^h_{\text{int}}$ in equation (3.52) is not valid for plasticity, since the constitutive equation in (2.8) has been used for its derivation. To obtain this expression, as for the non-symmetric discontinuous Galerkin method, for a given infinetly small increment expression (4.14) will be considered. For $\hat{\boldsymbol{u}}$ the numerical fluxes appearing in equations (3.1) and (3.2) will be used. An infinetly small increment of these numerical fluxes will be considered and due to their linear properties of the average operators,

$$\dot{\hat{\boldsymbol{u}}} = \left\{\dot{\boldsymbol{u}}^h\right\} \qquad \text{on } \tilde{\Gamma} \cup \Gamma^N, \tag{4.35}$$

$$\dot{\hat{\boldsymbol{u}}} = \boldsymbol{0} \qquad \text{on } \Gamma^D. \tag{4.36}$$

Inserting equations (4.35) and (4.36) into equation (4.14),

$$\int_{\tilde{\Omega}} \nabla^s \boldsymbol{\omega}^h : \dot{\boldsymbol{\sigma}}^h d\Omega = \int_{\tilde{\Omega}} \nabla^s \boldsymbol{\omega}^h : \mathbf{C}^{\text{ep}} : \nabla^s \dot{\boldsymbol{u}}^h d\Omega$$
$$- \int_{\tilde{\Gamma}} \left\{\nabla^s \boldsymbol{\omega}^h : \mathbf{C}^{\text{ep}}\right\} \boldsymbol{n}_K \cdot \left[\!\left[\dot{\boldsymbol{u}}^h\right]\!\right] d\Gamma. \tag{4.37}$$

Note that for the IP method and unlike the non-symmetric dG method, equation (4.18), an expression of the stresses in $\tilde{\Omega}$ depending on two components is obtained,

$$\dot{\boldsymbol{\sigma}}^h = \mathbf{C}^{\text{ep}} : \nabla^s \dot{\boldsymbol{u}}^h + \mathbf{C}^{\text{ep}} : \boldsymbol{R}\left(\left[\!\left[\dot{\boldsymbol{u}}^h\right]\!\right]\right) \qquad \text{in } \tilde{\Omega}, \tag{4.38}$$

where $\boldsymbol{R}(\cdot)$, defined in equation (3.51), is the lifting operator,

$$\int_{\tilde{\Omega}} \nabla^s \boldsymbol{\omega}^h : \mathbf{C}^{\text{ep}} : \boldsymbol{R}\left(\left[\!\left[\dot{\boldsymbol{u}}^h\right]\!\right]\right) d\Omega = -\int_{\tilde{\Gamma}} \left\{\nabla^s \boldsymbol{\omega}^h : \mathbf{C}^{\text{ep}}\right\} \boldsymbol{n}_K \cdot \left[\!\left[\dot{\boldsymbol{u}}^h\right]\!\right] d\Gamma. \tag{4.39}$$

The first component of the stress rate, which is called $\dot{\boldsymbol{\sigma}}^h_{\text{int}}$, is the same that can be found in the continuous case and it comes from the deformation of the interior of the elements,

$$\dot{\boldsymbol{\sigma}}^h_{\text{int}} = \mathbf{C}^{\text{ep}} : \nabla^s \dot{\boldsymbol{u}}^h. \tag{4.40}$$

The second component, called $\dot{\boldsymbol{\sigma}}^h_{\text{bound}}$, comes from the jump on the interior boundaries $\tilde{\Gamma}$, and it is equal to,

$$\dot{\boldsymbol{\sigma}}^h_{\text{bound}} = \mathbf{C}^{\text{ep}} : \boldsymbol{R}\left(\left[\!\left[\dot{\boldsymbol{u}}^h\right]\!\right]\right). \tag{4.41}$$

Using this notation and equation (4.38) the stress rate over $\tilde{\Omega}$ can be rewritten as,

$$\dot{\boldsymbol{\sigma}}^h = \dot{\boldsymbol{\sigma}}^h_{\text{int}} + \dot{\boldsymbol{\sigma}}^h_{\text{bound}}. \tag{4.42}$$

With equation (4.37) but now considering small finite increments,

$$\int_{\tilde{\Omega}} \nabla^s \boldsymbol{\omega}^h : \mathrm{d}\boldsymbol{\sigma}^h d\Omega = \int_{\tilde{\Omega}} \nabla^s \boldsymbol{\omega}^h : \mathrm{d}\boldsymbol{\sigma}^h_{\text{int}}\, d\Omega - \int_{\tilde{\Gamma}} \left\{\nabla^s \boldsymbol{\omega}^h : \mathbf{C}^{\text{ep}}\right\} \boldsymbol{n}_K \cdot \left[\!\left[\mathrm{d}\boldsymbol{u}^h\right]\!\right] d\Gamma. \tag{4.43}$$

This equation can be expressed in a non-incremental way by adding a total of k increments,

$$\int_{\tilde{\Omega}} \nabla^s \boldsymbol{\omega}^h : \boldsymbol{\sigma}^h d\Omega \simeq \int_{\tilde{\Omega}} \nabla^s \boldsymbol{\omega}^h : \boldsymbol{\sigma}^h_{\text{int}}\, d\Omega - \sum_{i=1}^{k} \int_{\tilde{\Gamma}} \left\{\nabla^s \boldsymbol{\omega}^h : \mathbf{C}^{\text{ep (i)}}\right\} \boldsymbol{n}_K \cdot \left[\!\left[\mathrm{d}\boldsymbol{u}^{h\,(i)}\right]\!\right] d\Gamma, \tag{4.44}$$

where it cannot be said that the last term of the right hand side of the above expression is equal to,

$$\sum_{i=1}^{k} \int_{\tilde{\Gamma}} \left\{\nabla^s \boldsymbol{\omega}^h : \mathbf{C}^{\text{ep (i)}}\right\} \boldsymbol{n}_K \cdot \left[\!\left[\mathrm{d}\boldsymbol{u}^{h\,(i)}\right]\!\right] d\Gamma \neq \int_{\tilde{\Gamma}} \left\{\nabla^s \boldsymbol{\omega}^h : \mathbf{C}^{\text{ep (i)}}\right\} \boldsymbol{n}_K \cdot \left[\!\left[\boldsymbol{u}^h\right]\!\right] d\Gamma, \tag{4.45}$$

because the value of $\mathbf{C}^{\text{ep (i)}}$ is not constant in every iteration. Note in equation (4.44) that the expression of $\boldsymbol{\sigma}^h$ as a function of $\boldsymbol{\sigma}^h_{\text{int}}$ and $\mathrm{d}\boldsymbol{u}^{h\,(i)}$ is not exact since the component associated to $\boldsymbol{\sigma}^h_{\text{bound}}$ has been obtained from an addition of displacements increments.

Finally the weak form in equation (4.34) can be obtained as a function of $\boldsymbol{\sigma}^h_{\text{int}}$ by introducing equation (4.44) into equation (4.34),

$$\begin{aligned}\int_{\tilde{\Omega}} \nabla^s \boldsymbol{\omega}^h : \boldsymbol{\sigma}^h_{\text{int}}\, d\Omega - \sum_{i=1}^{k} \int_{\tilde{\Gamma}} \left\{\nabla^s \boldsymbol{\omega}^h : \mathbf{C}^{\text{ep (i)}}\right\} \boldsymbol{n}_K \cdot \left[\!\left[\mathrm{d}\boldsymbol{u}^{h\,(i)}\right]\!\right] d\Gamma - \int_{\tilde{\Gamma}} \left[\!\left[\boldsymbol{\omega}^h\right]\!\right] \cdot \left\{\boldsymbol{\sigma}^h_{\text{int}}\right\} \boldsymbol{n}_K d\Gamma \\ + \int_{\tilde{\Gamma}} \left[\!\left[\boldsymbol{\omega}^h\right]\!\right] \frac{\eta_K}{h_K} \boldsymbol{D} \left[\!\left[\boldsymbol{u}^h\right]\!\right] d\Gamma = \int_{\tilde{\Omega}} \boldsymbol{\omega}^h \cdot \boldsymbol{f} d\Omega + \int_{\Gamma^N} \boldsymbol{\omega}^h \cdot \boldsymbol{g}^N d\Gamma.\end{aligned} \tag{4.46}$$

This is finally the non-linear equation that needs to be solved through an incremental iterative procedure.

4.2.2. Spatial discretization of interior penalty method

As done in Section 4.1.2, and using the notations introduced in Section 3.5, the expression of the weak form of the IP method in equation (4.46) can be discretized for the interface element in figure 3.1 as,

$$\begin{aligned}
&\int_{K_1} (\mathbf{B}_{e_1})^T \boldsymbol{\sigma}^h_{e_1\,\text{int}}\, d\Omega + \int_{K_2} (\mathbf{B}_{e_2})^T \boldsymbol{\sigma}^h_{e_2\,\text{int}}\, d\Omega - \sum_{i=1}^{k} \int_{\tilde{\Gamma}} \mathbf{B}_o^{\{\mathbf{C}^{\text{ep}}\}} \mathbf{N}_o^{[\![\,]\!]} \Delta \mathbf{a}_o^{(i)} d\Gamma \\
&- \int_{\tilde{\Gamma}} \left(\mathbf{N}_o^{[\![\,]\!]}\right)^T \left\{\boldsymbol{\sigma}^h_{\text{int}}\right\} \boldsymbol{n}_K d\Gamma + \int_{\tilde{\Gamma}} \left(\mathbf{N}_o^{[\![\,]\!]}\right)^T \frac{\eta_K}{h_K} \boldsymbol{D}\, \mathbf{N}_o^{[\![\,]\!]} \mathbf{a}_o\, d\Gamma \\
&\qquad = \int_{K_1} (\mathbf{N}_{e_1})^T \boldsymbol{f} d\Omega + \int_{K_2} (\mathbf{N}_{e_2})^T \boldsymbol{f} d\Omega + \int_{\Gamma^N} (\mathbf{N}_e)^T \boldsymbol{g}^N d\Gamma, \quad (4.47)
\end{aligned}$$

where $\mathbf{B}_o^{\{\mathbf{C}^{\text{ep}}\}}$ has been defined in equation (4.25). From there $\mathbf{F}_{\text{int}}$ can be found,

$$\begin{aligned}
\mathbf{F}_{\text{int}} \simeq &\int_{K_1} (\mathbf{B}_{e_1})^T \boldsymbol{\sigma}^h_{e_1\,\text{int}}\, d\Omega + \int_{K_2} (\mathbf{B}_{e_2})^T \boldsymbol{\sigma}^h_{e_2\,\text{int}}\, d\Omega - \sum_{i=1}^{k} \int_{\tilde{\Gamma}} \mathbf{B}_o^{\{\mathbf{C}^{\text{ep}}\}} \mathbf{N}_o^{[\![\,]\!]} \Delta \mathbf{a}_o^{(i)} d\Gamma \\
&- \int_{\tilde{\Gamma}} \left(\mathbf{N}_o^{[\![\,]\!]}\right)^T \left\{\boldsymbol{\sigma}^h_{\text{int}}\right\} \boldsymbol{n}_K d\Gamma + \int_{\tilde{\Gamma}} \left(\mathbf{N}_o^{[\![\,]\!]}\right)^T \frac{\eta_K}{h_K} \boldsymbol{D}\, \mathbf{N}_o^{[\![\,]\!]} \mathbf{a}_o\, d\Gamma. \quad (4.48)
\end{aligned}$$

A new term has been added compared to expression (4.5). This new term, as will be seen in the following section restores symmetry to the method.

$\mathbf{F}_{\text{ext}}$ remains unchanged, see equation (4.6),

$$\mathbf{F}_{\text{ext}} = \int_{K_1} (\mathbf{N}_{e_1})^T \boldsymbol{f} d\Omega + \int_{K_2} (\mathbf{N}_{e_2})^T \boldsymbol{f} d\Omega + \int_{\Gamma^N} (\mathbf{N}_e)^T \boldsymbol{g}^N d\Gamma. \quad (4.49)$$

The weak form in equation (4.34) can finally be expressed as a global equilibrium expression as done in (4.4), as a function of $\mathbf{F}_{\text{int}}$ and $\mathbf{F}_{\text{ext}}$,

$$\mathbf{F}_{\text{ext}} - \mathbf{F}_{\text{int}} = 0. \quad (4.50)$$

4.2.3. Linearization of interior penalty method

The solution is again found through an incremental-iterative procedure with the same steps as in Section 4.1.3.

1. Update the displacements and the strains given a trial nodal displacement over $\tilde{\Gamma}$ and on $\tilde{\Gamma}$,

$$\begin{aligned}
\mathbf{a}_e^{(k+1)} &= \mathbf{a}_e^{(k)} + \Delta \mathbf{a}_e^{(k+1)}, & (4.51)\\
\boldsymbol{\varepsilon}^{(k+1)}_{e\,\text{int}} &= \mathbf{B}_e \mathbf{a}_e^{(k+1)}, & (4.52)\\
\boldsymbol{\varepsilon}^{(k+1)}_{\partial K\,\text{int}} &= \mathbf{B}_e|_{\partial K} \mathbf{a}_e^{(k+1)}. & (4.53)
\end{aligned}$$

2. Given the strain field, $\boldsymbol{\varepsilon}^{(k+1)}_{e\,\text{int}}$, the plastic strain $\boldsymbol{\varepsilon}_e^{p\ (k+1)}$ and hardening variables $\boldsymbol{q}_e^{(k+1)}$, the corresponding stress is computed for each quadrature point using a classical return mapping algorithm. However the stress appearing in the weak form in equation

(4.46) is not, as in Section 4.1.3, the total stress. It is only the stress corresponding to what was called the interior part $\boldsymbol{\sigma}_{e\,\text{int}}^{(k+1)}$ of $\boldsymbol{\sigma}_{e}^{(k+1)}$. To obtain $\boldsymbol{\sigma}_{e\,\text{int}}^{(k+1)}$ only $\varepsilon_{e\,\text{int}}^{h}$ will be calculated and introduced in the return mapping algorithm. The strain that comes from the jump, $\boldsymbol{R}\left(\left[\!\left[\boldsymbol{u}^{h}\right]\!\right]\right)$, has not been considered. However it will be seen in Section 4.3 that even when low penalty values are used and the contribution of $\boldsymbol{R}\left(\left[\!\left[\boldsymbol{u}^{h}\right]\!\right]\right)$ to the total strain is larger, the method yields acceptable results. Bear in mind that the dG method is an approximate method, and will converge to the real solution as the number of elements and the penalty values are increased if the method is consistent and stable, which is the case here.

The same is done in ∂K_1 and ∂K_2 with $\boldsymbol{\varepsilon}_{\partial K}^{(k+1)}$, $\boldsymbol{\varepsilon}_{\partial K}^{p\,(k+1)}$ and $\boldsymbol{q}_{\partial K}^{(k+1)}$ to obtain $\boldsymbol{\sigma}_{\partial K\,\text{int}}^{(k+1)}$.

3. With $\boldsymbol{\sigma}_{e\,\text{int}}^{(k+1)}$, $\boldsymbol{\sigma}_{\partial K\,\text{int}}^{(k+1)}$ and $\mathbf{a}_{o}^{(k+1)}$, $\mathbf{F}_{\text{int}}^{(k+1)}$ is evaluated with equation (4.48).
4. For the given load level, $\boldsymbol{f}^{\,(n)}$ and $\boldsymbol{g}^{N\,(n)}$, $\mathbf{F}_{\text{ext}}^{(n)}$ is evaluated using (4.49).
5. Check if equilibrium equation, in (4.50) is satisfied. If this is the case the solution for the actual loading level is found. If this is not the case go to step six.
6. Calculate the next displacement increment, and set $k+1$ equal to k and go back to one.

Again it is the last step the one that has not been explained yet. To solve this, equation (4.48) is again linearized and then introduced in the global equilibrium equation (4.50),

$$\mathbf{F}_{\text{ext}}^{(n)} - \mathbf{F}_{\text{int}}^{(k)} - \frac{\partial \mathbf{F}_{\text{int}}}{\partial \mathbf{a}^{(k+1)}} \Delta \mathbf{a}^{(k+1)} = 0, \tag{4.54}$$

where,

$$\begin{aligned}\frac{\partial \mathbf{F}_{\text{int}}}{\partial \mathbf{a}_{e}^{(k+1)}} \Delta \mathbf{a}_{e}^{(k+1)} \simeq & \int_{K_1} \left(\mathbf{B}_{e_1}\right)^{T} \frac{\partial \boldsymbol{\sigma}_{e_1\,\text{int}}^{h}}{\partial \mathbf{a}_{e_1}^{(k+1)}} \Delta \mathbf{a}_{e_1}^{(k+1)} d\Omega + \int_{K_2} \left(\mathbf{B}_{e_2}\right)^{T} \frac{\partial \boldsymbol{\sigma}_{e_2\,\text{int}}^{h}}{\partial \mathbf{a}_{e_2}^{(k+1)}} \Delta \mathbf{a}_{e_2}^{(k+1)} d\Omega \\ & - \sum_{i=1}^{k} \int_{\tilde{\Gamma}} \mathbf{B}_{o}^{\{\mathbf{C}^{\text{ep}}\}} \mathbf{N}_{o}^{[\![\,]\!]} \frac{\partial \Delta \mathbf{a}_{o}^{(i)}}{\partial \mathbf{a}_{o}^{(k+1)}} \Delta \mathbf{a}_{o}^{(k+1)} d\Gamma - \int_{\tilde{\Gamma}} \left(\mathbf{N}_{o}^{[\![\,]\!]}\right)^{T} \frac{\partial \left(\left\{\boldsymbol{\sigma}_{\text{int}}^{h}\right\} \boldsymbol{n}_{K}\right)}{\partial \mathbf{a}_{o}^{(k+1)}} \Delta \mathbf{a}_{o}^{(k+1)} d\Gamma \\ & + \int_{\tilde{\Gamma}} \left(\mathbf{N}_{o}^{[\![\,]\!]}\right)^{T} \frac{\eta_K}{h_K} \boldsymbol{D}\, \mathbf{N}_{o}^{[\![\,]\!]} \frac{\partial \mathbf{a}_{o}}{\partial \mathbf{a}_{o}^{(k+1)}} \Delta \mathbf{a}_{o}^{(k+1)}\, d\Gamma. \end{aligned} \tag{4.55}$$

Note that now, from equation (4.38) and (4.42),

$$\dot{\boldsymbol{\sigma}}_{\text{int}}^{h} = \mathbf{C}^{\text{ep}} : \nabla \dot{\boldsymbol{u}}^{h} \qquad \text{in } \tilde{\Omega}. \tag{4.56}$$

The first and the second term of the right hand side of the discretized equation (4.55), as done in (4.22) now yield,

$$\int_{K_1} \left(\mathbf{B}_{e_1}\right)^{T} \frac{\partial \boldsymbol{\sigma}_{e_1\,\text{int}}^{h}}{\partial \mathbf{a}_{e_1}^{(k+1)}} \Delta \mathbf{a}_{e_1}^{(k+1)} d\Omega = \int_{K_1} \left(\mathbf{B}_{e_1}\right)^{T} \mathbf{C}_{e_1}^{\text{ep}} \mathbf{B}_{e_1}\, d\Omega\, \Delta \mathbf{a}_{e_1}^{(k+1)}, \tag{4.57}$$

and the third term follows directly as,

$$\sum_i \int_{\tilde{\Gamma}} \mathbf{B}_o^{\{\mathbf{C}^{\mathrm{ep}}\}} \mathbf{N}_o^{[\![\,]\!]} \frac{\partial \Delta \mathbf{a}_o^{(i)}}{\partial \mathbf{a}_o^{(k+1)}} \Delta \mathbf{a}_o^{(k+1)} d\Gamma = \int_{\tilde{\Gamma}} \mathbf{B}_o^{\{\mathbf{C}^{\mathrm{ep}}\}} \mathbf{N}_o^{[\![\,]\!]} d\Gamma \; \Delta \mathbf{a}_o^{(k+1)}. \tag{4.58}$$

To linearize the forth term of the right hand side of expression (4.55), it is done as in equation (4.25),

$$\int_{\tilde{\Gamma}} \left(\mathbf{N}_o^{[\![\,]\!]} \right)^T \frac{\partial \left(\left\{ \boldsymbol{\sigma}_{\mathrm{int}}^h \right\} \boldsymbol{n}_K \right)}{\partial \mathbf{a}_o^{(k+1)}} \Delta \mathbf{a}_o^{(k+1)} d\Gamma = \int_{\tilde{\Gamma}} \left(\mathbf{N}_o^{[\![\,]\!]} \right)^T \mathbf{B}_o^{\{\mathbf{C}^{\mathrm{ep}}\}} d\Gamma \; \Delta \mathbf{a}_o^{(k+1)}, \tag{4.59}$$

and with the last term of equation (4.55), see (4.26),

$$\int_{\tilde{\Gamma}} \left(\mathbf{N}_o^{[\![\,]\!]} \right)^T \frac{\eta_K}{h_K} \boldsymbol{D} \, \mathbf{N}_o^{[\![\,]\!]} \frac{\partial \mathbf{a}_o}{\partial \mathbf{a}_o^{(k+1)}} \Delta \mathbf{a}_o^{(k+1)} \, d\Gamma = \int_{\tilde{\Gamma}} \left(\mathbf{N}_o^{[\![\,]\!]} \right)^T \frac{\eta_K}{h_K} \boldsymbol{D} \, \mathbf{N}_o^{[\![\,]\!]} d\Gamma \; \Delta \mathbf{a}_o^{(k+1)}. \tag{4.60}$$

Finally to obtain $\Delta \mathbf{a}^{(k+1)}$, equation (4.54) is again considered,

$$\mathbf{K}^{(k+1)} \Delta \mathbf{a}^{(k+1)} = \mathbf{F}_{\mathrm{ext}}^{(n)} - \mathbf{F}_{\mathrm{int}}^{(k)}, \tag{4.61}$$

where from expression (4.55), (4.57), (4.58), (4.59) and (4.60),

$$\mathbf{K}_o^{(k+1)} = \begin{bmatrix} \int_{K_1} \mathbf{B}_{e_1}^T \mathbf{C}_{e_1}^{\mathrm{ep}} \, \mathbf{B}_{e_1} d\Omega \\ \int_{K_2} \mathbf{B}_{e_2}^T \mathbf{C}_{e_2}^{\mathrm{ep}} \, \mathbf{B}_{e_2} d\Omega \end{bmatrix} - \int_{\tilde{\Gamma}} \mathbf{B}_o^{\{\mathbf{C}^{\mathrm{ep}}\}} \mathbf{N}_o^{[\![\,]\!]} d\Gamma - \int_{\tilde{\Gamma}} \left(\mathbf{N}_o^{[\![\,]\!]} \right)^T \mathbf{B}_o^{\{\mathbf{C}^{\mathrm{ep}}\}} d\Gamma + \int_{\tilde{\Gamma}} \left(\mathbf{N}_o^{[\![\,]\!]} \right)^T \frac{\eta_K}{h_K} \boldsymbol{D} \, \mathbf{N}_o^{[\![\,]\!]} d\Gamma, \tag{4.62}$$

and from equation (4.49)

$$\mathbf{F}_{\mathrm{ext}}^{(n)} = \begin{bmatrix} \int_{K_1} \left(\mathbf{N}_{e_1} \right)^T \boldsymbol{f}^{\,(n)} d\Omega \\ \int_{K_2} \left(\mathbf{N}_{e_2} \right)^T \boldsymbol{f}^{\,(n)} d\Omega \end{bmatrix} + \int_{\Gamma^N} \mathbf{N}_e^T \boldsymbol{g}^{N\,(n)} d\Gamma, \tag{4.63}$$

and finally from (4.48),

$$\mathbf{F}_{\mathrm{int}}^{(k)} \simeq \begin{bmatrix} \int_{K_1} \mathbf{B}_{e_1}^T \boldsymbol{\sigma}_{e_1}^{h\,(k)} \, d\Omega \\ \int_{K_2} \mathbf{B}_{e_2}^T \boldsymbol{\sigma}_{e_2}^{h\,(k)} \, d\Omega \end{bmatrix} - \sum_{i=1}^{k} \int_{\tilde{\Gamma}} \mathbf{B}_o^{\{\mathbf{C}^{\mathrm{ep}}\}} \mathbf{N}_o^{[\![\,]\!]} d\Gamma \; \Delta \mathbf{a}_o^{(i)} - \int_{\tilde{\Gamma}} \left(\mathbf{N}_o^{[\![\,]\!]} \right)^T \left\{ \boldsymbol{\sigma}^{h\,(k)} \right\} d\Gamma + \int_{\tilde{\Gamma}} \left(\mathbf{N}_o^{[\![\,]\!]} \right)^T \frac{\eta_K}{h_K} \boldsymbol{D} \, \mathbf{N}_o^{[\![\,]\!]} d\Gamma \; \mathbf{a}_o^{(k)} \tag{4.64}$$

The obtained method is again consistent, but now it is adjoint consistent and symmetric as well. Note however, that the linearization is not exact since the different increments of the symmetry terms are directly summed up in the second term of the right hand side of equation (4.64).

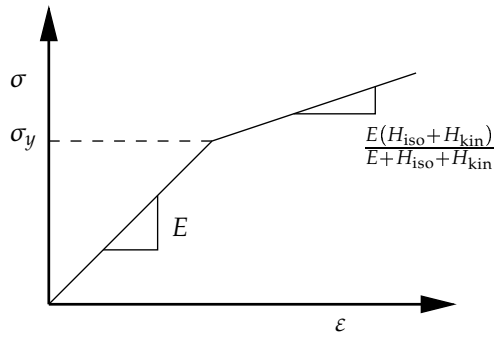

Figure 4.1. Plasticity model used.

4.3. Plasticity examples

4.3.1. One dimensional example

The example considered is the same used in the elasticity case in figure 3.4. However, now plasticity will be assumed using the linear hardening model, as appearing in figure 4.1, with the material parameters taken as,

$$\begin{aligned} E &= 1\ N/m^2, \\ H_{\text{iso}} &= 1/3\ N/m^2, \\ H_{\text{kin}} &= 1/3\ N/m^2, \\ \sigma_y &= 1\ N/m^2, \end{aligned} \tag{4.65}$$

where H_{iso} is the isotropic hardening modulus, H_{kin} the kinematic hardening modulus and σ_y the yield stress.

For the plasticity case an analytical solution is not known. To determine the convergence rate a benchmark is needed to which the obtained results can be obtained. For this purpose the numerical solution using 1000 continuous quadratic elements has been calculated.

Two different discontinuous methods will be analyzed. The non-symmetric discontinuous Galerkin method derived in Section 4.1 and the IP method, derived for plasticity in Section 4.2.

As stated before the used values of $\boldsymbol{D}$ appear in equation (3.40) for the one dimensional case and in (3.47) for two dimensions.

Non-symmetric discontinuous Galerkin method

The results obtained for the non-symmetric discontinuous Galerkin method can be seen in figure 4.2. The displacement calculated with traditional continuous Galerkin method is plotted in black. In figure 4.2(a) the discontinuous solution for linear elements using

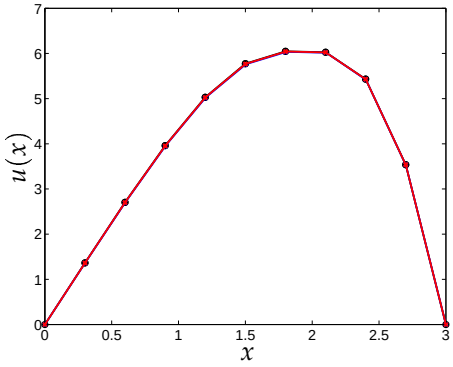

(a) In black cG, in blue dG $\eta_K = 2$ and in red $\eta_K = 5$ for 10 linear elements.

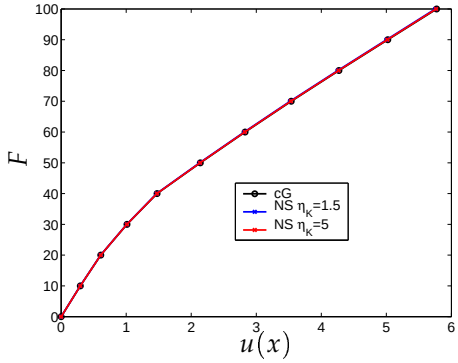

(b) Plastic response using linear elements for $x = 1.2\ m$.

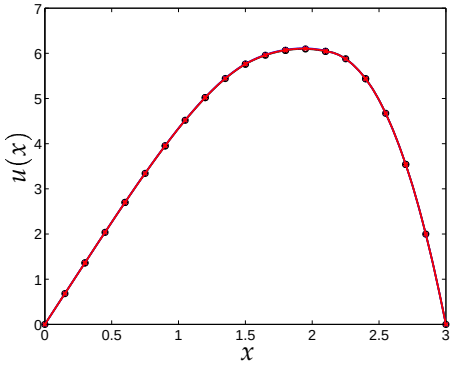

(c) In black cG, in blue dG $\eta_K = 5$ and in red $\eta_K = 10$ for 10 quadratic elements.

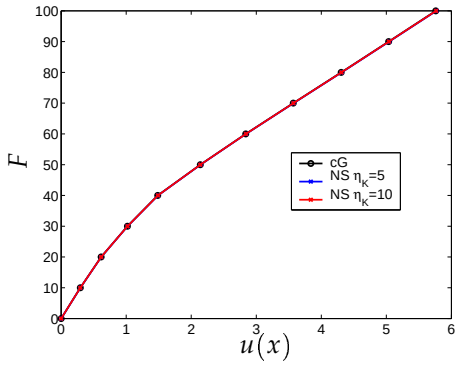

(d) Plastic response using quadratic elements for $x = 1.2\ m$.

Figure 4.2. Non-symmetric method for different values of η_K.

$\eta_K = 1.5$ is plotted in blue, while in red the solution for $\eta_K = 5$ is shown. In figure 4.2(c) quadratic elements are used. In blue the solution is plotted for $\eta_K = 5$ and in red for $\eta_K = 10$.

Figures 4.2(b) and 4.2(d) show the displacement of the midpoint section, $x = 1.5\ m$, of the considered example under increasing load using linear and quadratic elements respectively. See that it is not until 20% of the load is applied that plastic flow begins. The plastic response using linear and quadratic elements is plotted again with the same colors as in figures 4.2(a) and 4.2(c), respectively.

In figure 4.3 the rate of convergence can be seen for linear and quadratic elements. Note that the rate of convergence is approximately optimal for the considered values of η_K. However, the main problem associated with the resulting method is that it is not symmetric.

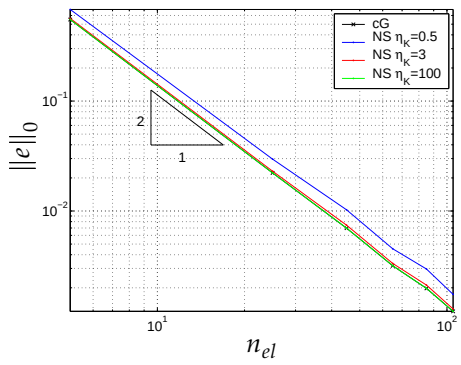

(a) Error in displacement using linear elements.

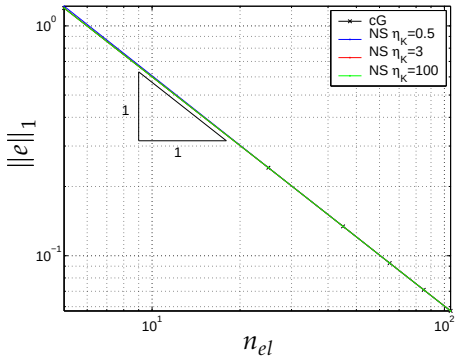

(b) Error in stresses using linear elements.

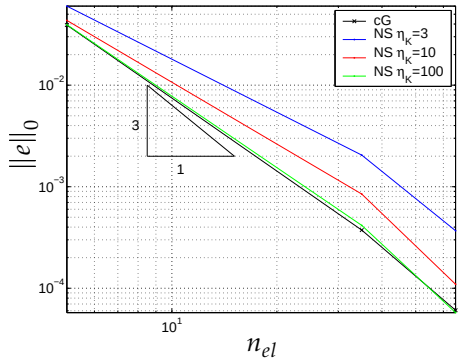

(c) Error in displacement using quadratic elements.

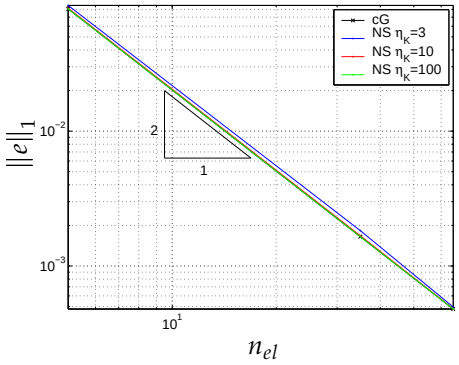

(d) Error in stresses using quadratic elements.

Figure 4.3. Error for non-symmetric discontinuous method using linear and quadratic elements.

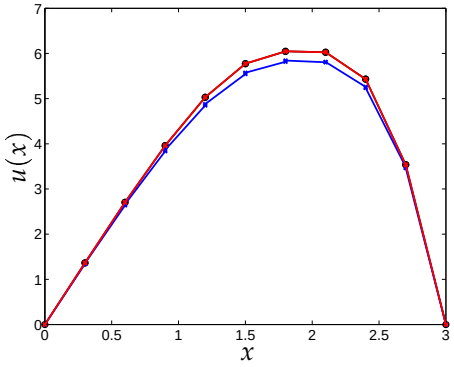

(a) In black cG, in blue dG $\eta_K = 2$ and in red $\eta_K = 5$ for 10 linear elements.

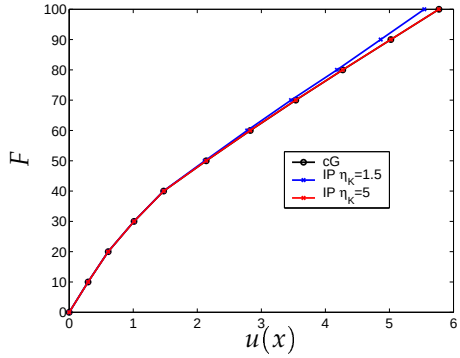

(b) Plastic response using linear elements for $x = 1.2\ m$.

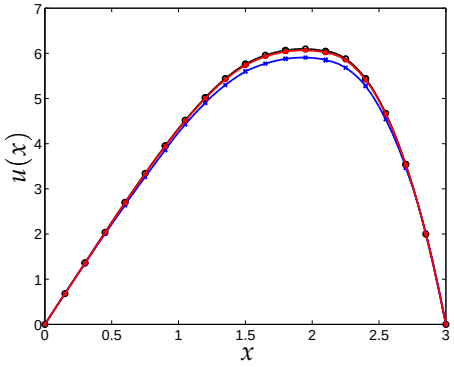

(c) In black cG, in blue dG $\eta_K = 5$ and in red $\eta_K = 10$ for 10 quadratic elements.

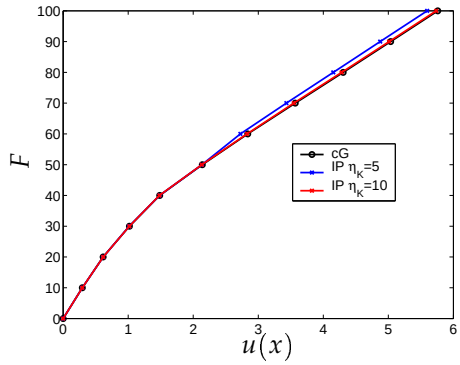

(d) Plastic response using quadratic elements for $x = 1.2\ m$.

Figure 4.4. Interior penalty method for different values of η_K.

Interior penalty method

The results obtained for the same example and values as used in Section 4.3.1 but now using the interior penalty method can be seen in figure 4.4.

In figure 4.4 a certain deterioration of the results can be seen compared to the non-symmetric method for the same values of η_K. This is because the strain used in the return mapping algorithm is evaluated only by means of the strain caused in the interior of the elements. The strain from the boundaries $\tilde{\Gamma}$ is not considered. Since there is a component of the stress missing in the IP case the level of yielding is not the same for the cG and the IP method. However, with a relatively low value of $\eta_K = 3$ in the linear case, figures 4.4(a) and 4.4(b), and $\eta_K = 10$ for the quadratic, figures 4.4(c) and 4.4(d), the results obtained are improved considerably.

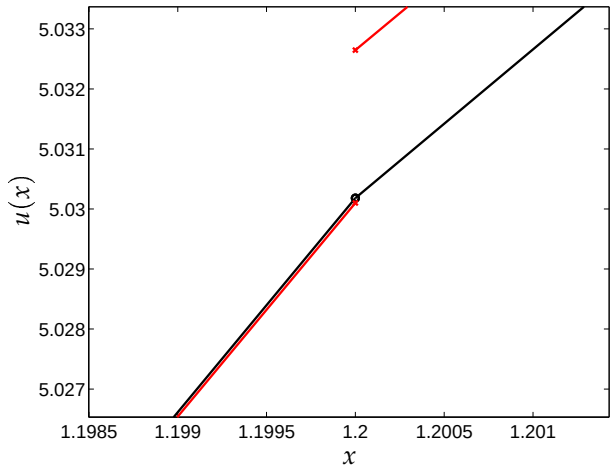

Figure 4.5. Detail of displacement for $x = 1.2\ m$ for interior penalty method with $\eta_K = 10$ using linear elements.

In figure 4.5 it can be seen that one of the properties of the IP method for the one dimensional elasticity case is lost. Note that the continuous solution cannot be obtained by calculating the average of the displacements of the IP method. This is caused by the reason explained before. If the jumps in the edges were considerably reduced so that the contribution to the total strain from the jump was very small in comparison to the contribution from the interior this property would be obtained again for plasticity.

The IP method however, even after not considering the component related to $\tilde{\Gamma}$ still converges, and as the value of η_K increases an optimal rate of convergence is obtained for displacements as well as stresses, figure 4.6. The difference with the non-symmetric method is that the IP method is now symmetric.

Unloading has also been tested for the two studied methods, interior penalty and non-symmetric discontinuous Galerkin method, considering ten linear elements yielding the results appearing in figure 4.7.

Another difference between the non-symmetric Galerkin method and the interior penalty method is the number of iterations needed to obtain a converged solution. Note that the linearization of the interior penalty method is not exact. The term giving symmetry to the method can then lead to unloading. This causes a larger number of iterations to reach convergence for the interior penalty method than for the non-symmetric discontinuous and the continuous Galerkin methods. In Table 4.1, the number of iterations used for the example in figure 3.4 is shown. The plasticity model adopted is the same as before, using a total number of ten linear elements. The stabilizing parameter is taken equal to $\eta_K = 10$ for both the interior penalty and the non-symmetric discontinuous Galerkin method. The load is applied in only one increment. The criterion used to guarantee convergence is the

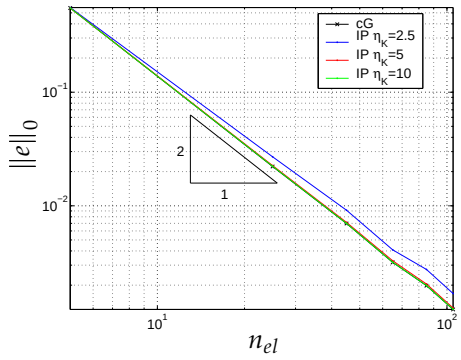

(a) Error in displacement using linear elements.

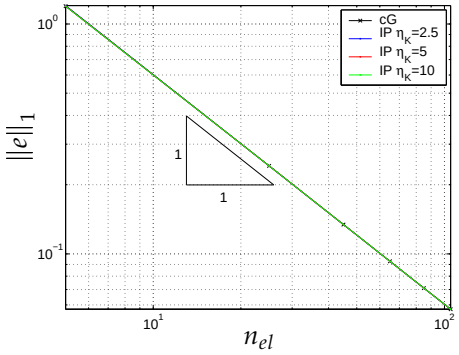

(b) Error in stresses using linear elements.

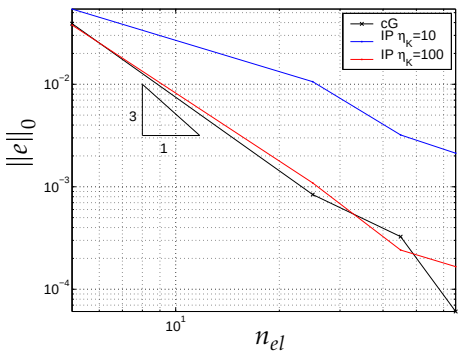

(c) Error in displacement using quadratic elements.

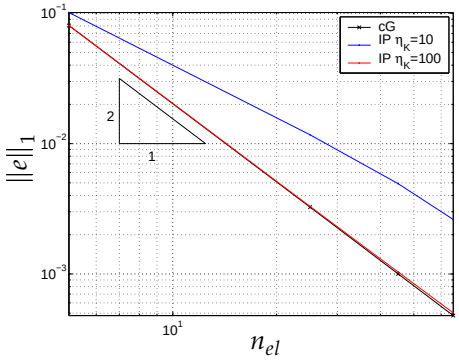

(d) Error in stresses using quadratic elements.

Figure 4.6. Error for interior penalty method using linear and quadratic elements.

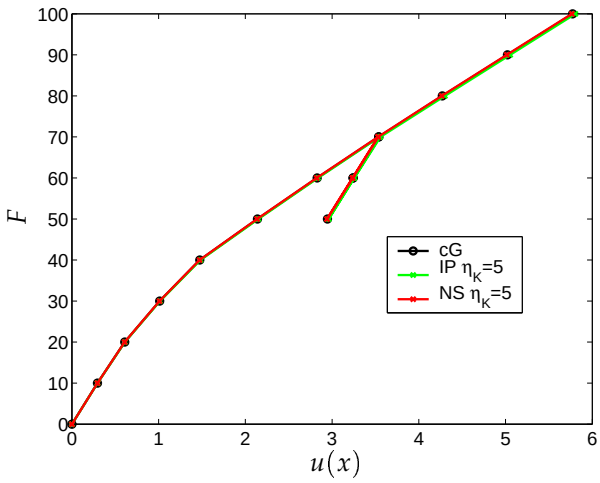

Figure 4.7. Unloading for examples in figure 4.4(b) and figure 4.2(b).

so-called force norm criterion. With this criterion iterations are added until the change in the norm of the unbalanced force vector is smaller than a prescribed value ε times the value of the unbalance force in the first iteration of the loading step [14],

$$\left\| \mathbf{F}_{\text{ext}}^{(n)} - \mathbf{F}_{\text{int}}^{(k)} \right\|_2 < \varepsilon \left\| \mathbf{F}_{\text{ext}}^{(n)} - \mathbf{F}_{\text{int}}^{(1)} \right\|_2, \tag{4.66}$$

where, as seen in Chapter 4, the superscript n stands for the increment step, in this case equal to one, and k stands for the iteration number. The choice of ε will be taken equal to $\varepsilon = 5 \times 10^{-10}$. So for each iteration in Table 4.1, the value of,

$$\frac{\left\| \mathbf{F}_{\text{ext}}^{(1)} - \mathbf{F}_{\text{int}}^{(k)} \right\|_2}{\left\| \mathbf{F}_{\text{ext}}^{(1)} - \mathbf{F}_{\text{int}}^{(1)} \right\|_2}, \tag{4.67}$$

is shown.

See how for the continuous Galerkin method and the non-symmetric discontinuous Galerkin method, the amount of iterations needed is equal to two, while for the interior penalty method, four iterations are needed. For the IP method in iteration number two and three there is a certain oscillation around the reached solution.

Iteration number k	cG	NS	IP
1	1	1	1
2	6.22×10^{-15}	7.79×10^{-14}	5.98×10^{-4}
3	–	–	2.56×10^{-4}
4	–	–	5.09×10^{-14}

Table 4.1. Iterations used to obtain convergence in the Newton scheme for the continuous Galerkin method (cG), non-symmetric discontinuous Galerkin method (NS) and interior penalty method (IP)

4.3.2. Two dimensional example

The example considered in this section is the same as in Section 3.7.3. However, now plasticity will be assumed using the following material properties,

$$\begin{aligned} F &= 5000\, N/mm, \\ L &= 1000\, mm, \\ h &= 50\, mm, \\ \nu &= 0.3, \\ E &= 210000\, N/mm^2, \\ H_{\text{iso}} &= 10000\, N/mm^2, \\ H_{\text{kin}} &= 0\, N/mm^2, \\ \sigma_y &= 240\, N/mm^2. \end{aligned} \tag{4.68}$$

Again the non-symmetric as well as the IP method will be considered. The solution for the non-symmetric method are given in figure 4.8 and for the IP method in 4.9.

The observed problems for the one dimensional case can be seen as well for two dimensions. The preference of the interior penalty method over the non-symmetric method in the elastic case changes in plasticity. As seen in Section 4.3.1 two are mainly the problems observed for the IP method. The first problem is related to the omission of the strain component $\varepsilon^h_{\text{bound}}$ in the return mapping algorithm, and the second related to the inexact linearization of the weak form. The first problem explains why the observed distortion occurs in figure 4.9(b), blue line for $\eta_K = 5$. It also explains why in figures 4.9(c) and 4.9(d) for a lower value of η_K the displacements are actually smaller than for a greater value of η_K, opposite to the observed behavior for elasticity.

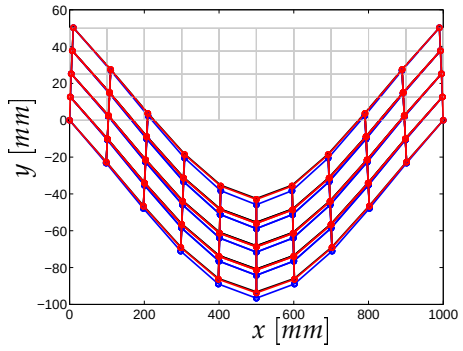

(a) Displacement of the beam in figure 3.13. In black cG, in blue non-symmetric dG with $\eta_K = 10$ and in red with $\eta_K = 100$.

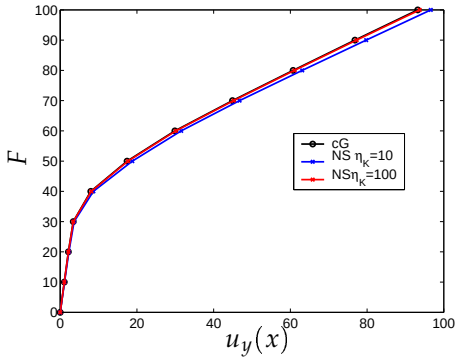

(b) Plastic response for $x = 500\ mm$. In black cG, in blue non-symmetric dG with $\eta_K = 10$ and in red with $\eta_K = 100$.

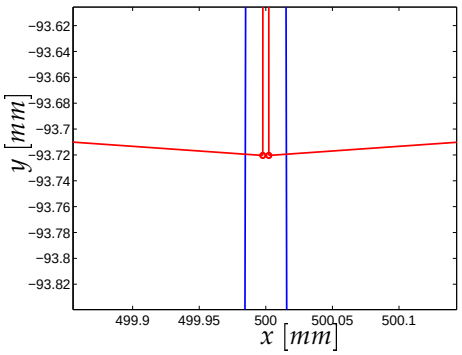

(c) Detail of figure 4.8(a).

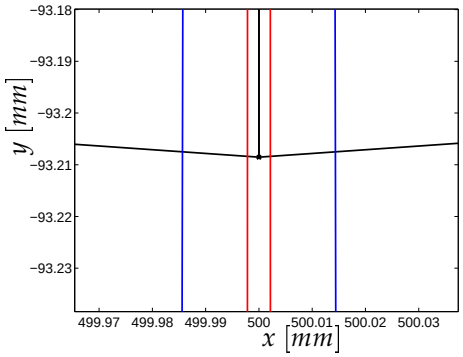

(d) Detail of figure 4.8(a).

Figure 4.8. Non-symmetric discontinuous Galerkin method two dimensions plane strain example.

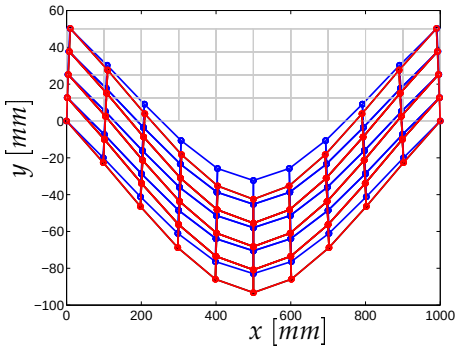

(a) Displacement of the beam in figure 3.13. In black cG, in blue IP method with $\eta_K = 10$ and in red with $\eta_K = 100$.

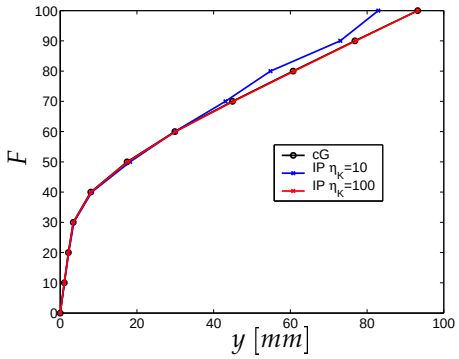

(b) Plastic response for $x = 500\ mm$. In black cG, in blue IP method with $\eta_K = 10$ and in red with $\eta_K = 100$.

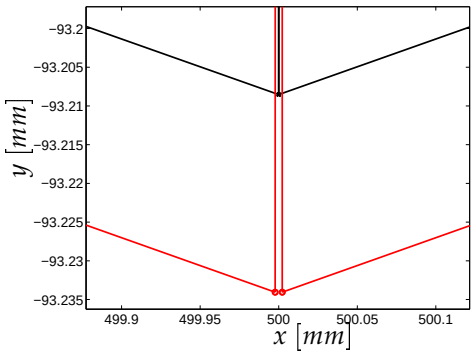

(c) Detail of figure 4.9(a).

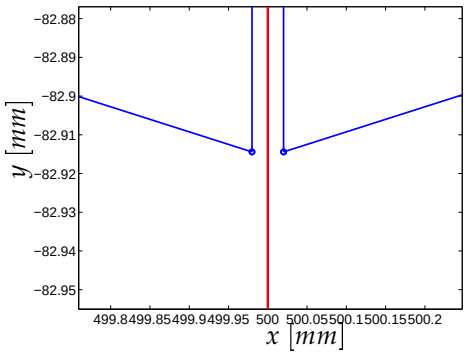

(d) Detail of figure 4.9(a).

Figure 4.9. Interior penalty method two dimensions plane strain example.